

Highly Efficient Human Action Recognition with Quantum Genetic Algorithm Optimized SVM

Yafeng Liu, Shimin Feng, Zhikai Zhao, Enjie Ding

In this paper we propose the use of quantum genetic algorithm to optimize the support vector machine (SVM) for human action recognition. The Microsoft Kinect sensor can be used for skeleton tracking, which provides the joints' position data. However, how to extract the motion features for representing the dynamics of a human skeleton is still a challenge due to the complexity of human motion. We present a highly efficient features extraction method for action classification, that is, using the joint angles to represent a human skeleton and calculating the variance of each angle during an action time window. Using the proposed representation, we compared the human action classification accuracy of two approaches, including the optimized SVM based on quantum genetic algorithm and the conventional SVM with cross validation. Experimental results on the MSR-12 dataset show that the conventional SVM achieved an accuracy of 93.85%. The proposed approach outperforms the conventional method with an accuracy of 96.15%. The classification accuracy is increased by 2.3%.

I. INTRODUCTION

Human action recognition (HAR) plays an important role in video surveillance, health care and human-computer interaction [1]. One goal of HAR is to provide the information about the user's behavior and make the computer system assist the user with the task. The recognition and prediction of elderly people's behavior will help them with their health care [2]. In HCI, human activity recognition plays a key role in natural interaction area. Moreover, HAR has been widely used in several fields, e.g. sports motion analysis, virtual reality (VR), augmented reality (AR) and other human-computer interaction area.

The research methods can be divided into two categories, including the video-based methods and the sensor-based methods [3]. The development of new sensing devices, e.g. the Microsoft Kinect and other RGB-D devices bring new opportunities for the HAR researchers [4]. This kind of devices are not expensive, portable, and can be used for skeleton tracking, which provide 15 – 20 joints' information. The action classification approaches mainly include decision tree, Bayes, KNN, NN, SVM, HMM, etc. The main drawback is the need for manual labelling. Human action recognition is a challenging task that have been addressed with different methods, such as SVM and DTW, by considering many different kinds of information, e.g. joint positions, key poses, joint angles. This paper presents an approach for action recognition that considers only the information extracted from the 3D skeletal joints. We extract the skeletal features by computing all angles between any triplet of joints and then calculate the variance of each angle during the time period when an action is performed. For classification, we use the Quantum Genetic Algorithm (QGA) to improve the performance of the SVM. We evaluate our approach on the Microsoft dataset and compare our results with the SVM cross validation results.

The human motion is complex and the pattern of human action is not easy to be described [5]. The Microsoft

Kinect can be used for skeleton tracking that provide us with lots of skeletal joints' data. The direct use of these data for HAR will significantly influence the recognition rate and the speed. How to process the high-dimensional data to reduce the redundancy of information is still a challenge. Besides, it is not an easy task to find the appropriate parameters for SVM due to the limited searching capability with the cross validation method. SVM is an easy and efficient supervised learning model, classifying n -dimensional samples through the $n-1$ dimensional hyperplane. One drawback of the traditional SVM is the inefficiency of parameter selection. Thus the best classification results can not be achieved. An inappropriate parameter will decrease the performance of SVM classifier. To solve these problems, we propose the use of joint angles to represent the human skeleton and an optimized SVM classification method based on the quantum genetic algorithm for human action classification. Essentially speaking, SVM is about searching for the best solution of the function. Therefore, under the condition of the same computing resources, it can search in a larger area, which allows the diversity of the sampling space. This helps ease the prematurity problem of the genetic algorithm.

According to the classical Newtonian mechanics theory, people can get the motion of the object completely when they know the initial state and driving force. But the behavior of human body is complex and there is a large number of interaction objects, this method does not work. Therefore, people focus on the theory of machine learning based on data driven. By studying the statistical laws and structural characteristics of the data, we can identify the characteristics of human behavior and predict the behavior. Several methods are commonly used, such as neural network, K-clustering method and support vector machine [6, 7]. Support vector machines are widely used because of their simplicity and efficiency. Support Vector Machine [8] classifies the data by constructing hyperplane, separating different categories of data from each other. However, the two parameters of

support vector machine, i.e. the penalty factor c and kernel function parameter σ affect the accuracy of classification to a great extent. Therefore, how to search for the optimal parameters is a key problem that support vector machines need to solve. For SVM parameter optimization, the researchers have tried different algorithms, among which the grid algorithm, the particle swarm algorithm and the genetic algorithm are three commonly used methods.

However, the simple mesh optimization algorithm is not ideal, and the particle swarm algorithm and genetic algorithm are easy to converge to local optimal solutions due to precocity. So we will use the quantum genetic algorithm to improve the efficiency of SVM parameter optimization. The quantum algorithm is based on the correlation [9–11] of quantum bits, which gives the algorithm the characteristics of parallelism. Compared with the classical algorithm, the computational efficiency has been greatly improved [11, 12]. In order to improve the search efficiency, the population search range of SVM parameters is enlarged. In recent years, the quantum genetic algorithms have been widely used in machine fault diagnosis, geology research and environmental analysis [13–17]. In this paper, we use the quantum genetic algorithm to optimize the SVM for classifying the human actions by considering the search efficiency of quantum genetic algorithm and building a better SVM classification model.

The rest of the paper is organized as follows. Section 2 presents the Kinect system and the classification algorithm. We describe the experimental results in Section 3 and concludes the paper in Section 4.

II. METHODS

A. Feature Extraction of Human Action

As shown in Figure 1(a), we get the 3D positions of each skeleton joint with the Kinect. The human action sample is defined as

$$\mathbf{f} = [\mathbf{f}_1, \mathbf{f}_2, \dots, \mathbf{f}_n, \dots, \mathbf{f}_{20}] \quad (1)$$

where \mathbf{f}_n is the coordinates of the n -th joint. As there are 20 joints, we get a 60-dimensional vector. In reality, we don't need an accurate joint position for human activity recognition as the relative positions will meet our requirements. We calculate the phasor difference of the two adjacent joints. This vector illustrates the direction of the limb between these two joints. For a joint connected with multiple limbs, the angles are formed, as shown in Figure 1(b).

Consider a skeleton joint and the two adjacent joints-

the coordinates are

$$\mathbf{f}_{n-1} = (x_{n-1}, y_{n-1}, z_{n-1}) \quad (2a)$$

$$\mathbf{f}_n = (x_n, y_n, z_n) \quad (2b)$$

$$\mathbf{f}_{n+1} = (x_{n+1}, y_{n+1}, z_{n+1}) \quad (2c)$$

The vector of the limb defined by two adjacent joints
The angle θ

$$\theta = \frac{\cos(\mathbf{a}, \mathbf{b})}{\|\mathbf{a}\| * \|\mathbf{b}\|} \quad (3)$$

As Fig. 1(a) shows, there are five joints which own only one junction (red points in Fig.1(a)), no angles exists on these joints. There are 13 joints which own two junctions (blue points in Fig.1(a)), and each of these joints owns one angle. There are only one joint which owns three junctions (yellow points in Fig.1(a)). According to the knowledge of permutation and combination, the angles on this joint are $C_3^2 = 3$ totally. At last, the shoulder center joint own four junctions. So there are $C_4^2 = 6$ angles on it. The total number of angles are $13 + 3 + 6 = 22$ on body joints.

The relationship between the skeleton joints and the angles is shown in Table I. The left column in the table shows the spatial position label of joints, and they are all three dimensional vector. The right column shows the the intersection angle label between limb, and all of them are scalars. These labels of angle sample are arranged according to their order of position sample. We can see that the dimensions of sample are reduced from 60 to 22 using angle strategy. However, there are two special joint, joint 1 and joint 3(see Fig.1(b)). More than one angles exist within these two joints. We define another ranking method here: we arrange angles within the same joints according to the order of joint label next to it. For example, the first joint, hip center, there are three connecting joints, which are the 2nd, the 13th and the 17th joint. As Fig. 1(b), we name the angle formed by joint 2 and joint 13 θ_1 , the angle formed by joint 2 and joint 17 θ_2 , and the joint formed by joint 13 and 17 θ_3 . For joint 3, we use the same method. The joints connecting to the joint 3 are the 2nd, 4th, 5th and 9th joint, so we name the angle formed by joint 2 and joint 4 θ_5 , the angle formed by joint 2 and joint 5 θ_6 , the angle formed by joint 2 and joint 9 θ_7 , the angle formed by joint 4 and joint 5 θ_8 , the angle formed by joint 4 and joint 9 θ_9 , and the angle formed by joint 5 and joint 9 θ_{10} .

As shown in Figure 1(a), there are 5 joints where there are no angles. There are 13 angles for the joints that are connected with two limbs. There is one joint that is connected with three limbs, thus there are $C_3^2 = 3$ angles according to the permutation and combination. There is one joint that is connected with four limbs, which gives $C_4^2 = 6$ angles. Therefore, the total number of the angles is $13 + 3 + 6 = 22$.

We use the angle representation method to reduce the 60-dimensional vector to 22-dimensional vector. For the

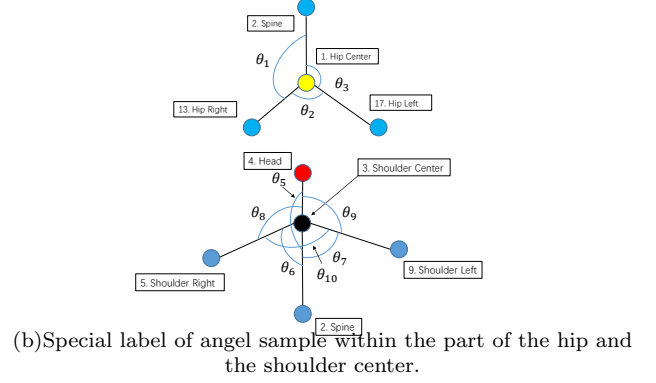
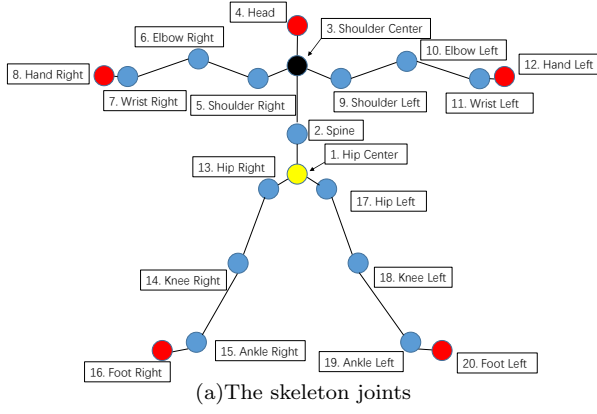


Figure 1. The schematic diagram of the skeleton joints

Table I. The corresponding relationship between the skeleton joints and the angles

The index of skeleton joints	The index of joint angles
1	$\theta_1, \theta_2, \theta_3$
2	θ_4
3	$\theta_5, \theta_6, \theta_7, \theta_8, \theta_9, \theta_{10}$
4	—
5	θ_{11}
6	θ_{12}
7	θ_{13}
8	—
9	θ_{14}
10	θ_{15}
11	θ_{16}
12	—
13	θ_{17}
14	θ_{18}
15	θ_{19}
16	—
17	θ_{20}
18	θ_{21}
19	θ_{22}
20	—

continuous action, we need to add the timing information and process multiple frames together for action recognition. Here we set a time window for action segmentation. Assume the action lasts for T s, during which period there are M frames acquired from the Kinect. We can get the variance of each angle in this time window.

$$j_n = \frac{1}{(M-1)} \sum_M^k (f_{nk} - \mu_n)^2 \quad (4)$$

B. Quantum Genetic Algorithm (QGA)

QGA is an optimization algorithm based on quantum computing theory. The quantum theory, the state vector is used to describe genetic coding, and use the quantum revolving gate to realize the evolution of population. Because of the parallelism of quantum algorithm, the quantum genetic algorithm is better than the traditional quantum algorithm in population size and searching speed.

The Coding of Quantum genetic algorithm. The binary and decimal codes are used in the classical genetic algorithm. When quantum bits are used, the encoding will be different. There is superposition and coherence between the quantum states, so unlike the classical bits, there are entanglement properties between different qubits. For a binary bit, qubits cannot simply be written as 0 or 1 states, but as an arbitrary superposition between them, so the qubit can be written as:

$$|\psi\rangle = \alpha|0\rangle + \beta|1\rangle \quad (5)$$

where $|0\rangle$ and $|1\rangle$ are both vectors, representing the system states. α and β are a pair of plural. They correspond to the probability amplitude of these two states. The square is the probability observed corresponding to these two states. The relationship satisfies the normalization rule:

$$|\alpha_i|^2 + |\beta_i|^2 = 1 \quad (6)$$

Thus, the pair $[\alpha, \beta]^T$ that satisfies 5 and 6 can be used to represent a quantum bit. A chromosome with m bits can be expressed as:

$$P_j = \begin{bmatrix} \alpha_1 & \alpha_2 & \cdots & \alpha_m \\ \beta_1 & \beta_2 & \cdots & \beta_m \end{bmatrix} \quad (7)$$

For each element of the chromosome, $|\alpha_i|^2 + |\beta_i|^2 = 1, i = 1, 2, \dots, m$

The Quantum Revolving Door. In the quantum genetic algorithm, the operation of quantum bits is achieved through the quantum logic revolving gate. The rotation of the quantum logic gate can help realize the evolution of the population. The optimal gene can be produced faster in the population through the guidance of optimization conditions. This can speed up the entire algorithm. The operation of a quantum logic gate can be expressed in the form of a matrix:

$$\begin{bmatrix} \alpha_i^{t+1} \\ \beta_i^{t+1} \end{bmatrix} = G \begin{bmatrix} \alpha_i^t \\ \beta_i^t \end{bmatrix} \quad (8)$$

where $[\alpha_i^t, \beta_i^t]$ and $[\alpha_i^{t+1}, \beta_i^{t+1}]$ represent the quantum bits of the chromosomes for the generation t and $t + 1$ respectively. G represents the quantum revolving door:

$$G = \begin{bmatrix} \cos \theta_i & -\sin \theta_i \\ \sin \theta_i & \cos \theta_i \end{bmatrix} \quad (9)$$

θ is the rotation speed. The selection of direction and magnitude is shown in Table II.

In table II, x_i and b_i represent the optimal chromosome and the current optimal chromosome in the current population, respectively. $f(x)$ is the fitness function, $\delta\theta$ is the rotation angle. By selecting different rotation angles, we can control the convergence speed. $S(\alpha_i, \beta_i)$ is the direction of the rotation angle.

C. Support Vector Machine

Support Vector Machine (SVM) can mainly be divided into two parts: classification and problem solving. It is widely used because of its high efficiency and simplicity in dealing with classification problems. It is a kind of supervised learning model, which describes the parameter space $x_k \in r^n$ of object corresponds to a label class space $y_k \in R$. This constitutes the sample data space $d = (X_k, y_k) | k = 1, 2, \dots, n$, N is the number of the samples. Support Vector machine is to find a set of hyperplane, which is composed of two parallel hyperplanes constructed by the nearest two points in the classification groups. In order to achieve the best classification results, we need to make the distance between the two sets of hyperplanes as large as possible.

As shown in Figure 2, the hyperplane represented by the solid line is constructed by the data-points, which are closet to the plane. The task of SVM is to find the maximum value of $2/|\omega|$. This optimization problem can be written as:

$$\min_{\omega, b} \psi(\omega, b) = \frac{1}{2} \omega^T \omega \quad (10)$$

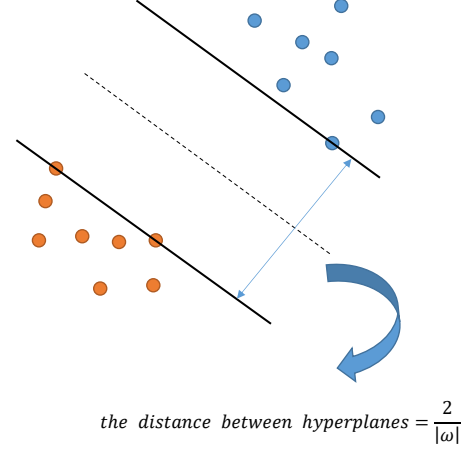


Figure 2. The diagram of the classification surface

where b is a biased function, which is included in the restriction condition $y_k(\omega^T \phi(x_k) + b) \geq 1$. The Lagrange equation can be obtained:

$$L(\omega, b, \lambda) = \psi(\omega, b) - \sum_{k=1}^N \lambda_k \{y_k(\omega^T \phi(x_k) + b) - 1\} \quad (11)$$

The parameters of SVM can be obtained by finding the extremum of the equation. However, for practical problems, the distance between two classes may not be so large. Thus, it is necessary to introduce the concept of soft interval classification, that is, to allow some points to fall between two of hyperplane, but not across the middle dotted line. In this case, the target function needs to add a slack variable and the constraint should be modified to $y_k(\omega^T \phi(x_k) + b) \geq 1 - \epsilon_k$, $\epsilon_k \geq 0$. This condition is not so strict as the previous constraint. The sample point may appear between the two hyperplanes. The corresponding dual equation can be modified to:

$$L(\omega, b, \epsilon, \lambda, \mu) = \psi(\omega, b) + C \sum_{k=1}^N \epsilon_k^n - \sum_{k=1}^N \lambda_k \{y_k(\omega^T \phi(x_k) + b) - 1 + \epsilon_k\} - \sum_{k=1}^N \mu_k \epsilon_k \quad (12)$$

In the ??, c is the penalty factor and n is a natural number, corresponding to the n -order soft interval classification. We set $n = 1$ here, which is the linear soft interval classification.

According to the optimization condition,

$$\frac{\partial L}{\partial \omega} = 0, \quad \frac{\partial L}{\partial b} = 0, \quad \frac{\partial L}{\partial \epsilon_k} = 0, \quad \frac{\partial L}{\partial \lambda_k} = 0 \quad (13)$$

Table II. The rotation strategy of the quantum revolving door.

x_j	$best_j$	$f(x) > f(best)$	$\Delta\theta_j$	$\alpha_j\beta_j > 0$	$\alpha_j\beta_j < 0$	$s(\alpha_j, \beta_j)$ $\alpha_j = 0$	$\beta_j = 0$
0	0	FALSE	0	0	0	0	0
0	0	TRUE	0	0	0	0	0
0	1	FALSE	0.01π	+1	-1	0	± 1
0	1	TRUE	0.01π	-1	+1	± 1	0
1	0	FALSE	0.01π	-1	+1	± 1	0
1	0	TRUE	0.01π	+1	-1	0	± 1
1	1	FALSE	0	0	0	0	0
1	1	TRUE	0	0	0	0	0

We get:

$$\left. \begin{aligned} \omega &= \sum_{k=1}^N \lambda_k y_k \phi(x_k) \\ \sum_{k=1}^N \lambda_k y_k &= 0 \\ C &= \lambda_k + \mu_k \\ y_k(\omega^T \phi(x_k) + b) - 1 + \epsilon_k &= 0 \end{aligned} \right\} \quad (14)$$

The extremum condition after derivation is brought back to Lagrange function. We get the simplified equation:

$$\max_{\lambda} \sum_{k=1}^N \lambda_k - \frac{1}{2} \sum_{i=1}^N \sum_{j=1}^N \lambda_i \lambda_j y_i y_j \phi(x_i) \phi(x_j) \quad (15)$$

In comparison with the conventional SVM, the constraint conditions are changed:

$$\sum_{k=1}^N \lambda_k y_k = 0 \quad (16)$$

$$0 \leq \lambda_k \leq C \quad k = 1, 2, \dots, N \quad (17)$$

It can be seen that the Lagrange coefficient is not simply set to a real number that is not less than 0 under the condition of soft interval classification. Its value is less than the penalty factor c .

When describing the parameters of the sample points, we do not use x_k directly, instead we use a mapping $\phi(X_k)$. This is due to the fact that we cannot get good classification results with a linear classification plane in many practical problems. We need a more complex plane to make the classification better. This kind of mapping plays such a role. In 15, we define $K(X_i, x_j) = \phi(x_i) \phi(x_j)$, where $k(X_i, x_j)$ is called the kernel function. The commonly used kernel functions can be divided into the following categories:

a. *Radial Basis Function*

$$K(x_i, x_j) = \exp(\|x_i - x_j\|^2 / \sigma^2) \quad (18)$$

b. *Polynomial Kernel Function*

$$K(x_i, x_j) = (x_i \cdot x_j + c)^d \quad (19)$$

c. *Sigmoid Kernel Function*

$$K(x_i, x_j) = \tan(k(x_i \cdot x_j) + v) \quad (20)$$

d. *Linear Kernel Function*

$$K(x_i, x_j) = x_i \cdot x_j \quad (21)$$

D. The Flowchart of the Algorithm

In order to make the support vector machine run normally, the penalty factor c and the kernel function parameter σ are two variables needed to be determined according to 15 ~ 21. These two variables will directly affect the accuracy of the classification. How to determine these two parameters quickly and accurately is the key to the successful SVM modeling. We will use the quantum genetic algorithm to optimize these two parameters. The flowchart is shown in Figure 3. It can be seen that the two parameters need to be encoded first. Then the optimal solution is constantly adjusted through the quantum revolving door operation. By initializing a set of parameters, the accuracy of classification is obtained. This accuracy is used as the fitness function. We aim to search out a set of (C, σ) with the highest correct rate.

The eight steps of the SVM based on QGA optimization algorithm

Step 1 Initialize the algorithm parameters, including the maximum number of iterations, population size, variable binary length and so on. Enter the training set data and test set data, as well as the corresponding labels.

Step 2 Initialization population $q(t)$: equal treatment of all genes, that is, initialize all genes $[\alpha_i^t, \beta_i^t]$ to $[1/\sqrt{2}, 1/\sqrt{2}]$, indicating that each chromosome appears equally in the initial search.

Step 3 Measure the initial population and set a fixed $p(t)$, which is a series of binary codes of the initialization length. It is transformed into the penalty factor and the parameters of kernel function. It is brought into the SVM model with the training sample to train the SVM. By testing the sample, we get the accuracy. The current individual is evaluated and the optimal individual is retained.

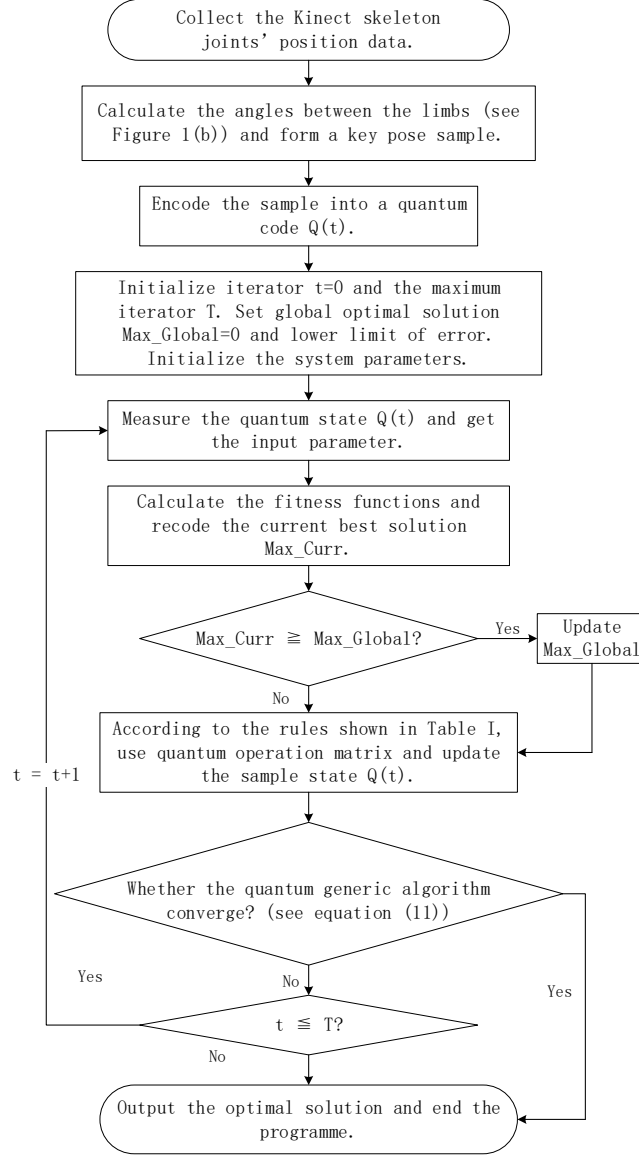


Figure 3. Flowchart

Step 4 Determine if precision is convergent or if the maximum number of iterations is reached. If yes, the algorithm terminates, else go to step 5.

Step 5 Update population $q(t)$ by using the rotation angle strategy in table II.

Step 6 Check to see whether the catastrophic conditions are met. If yes, keep the optimal value and initialize the population. If not, go to step 7.

Step 7 Increase the number of iterations by one and return to step 3 to continue the execution.

Step 8 Output the optimization parameters and evaluate the test samples with these parameters.

III. THE CLASSIFICATION PROCESS AND EXPERIMENT RESULTS

A. Problem Statement

We used the MSRC-12 gesture dataset [18], which consists of sequences of 12 groups of actions collected by the Cambridge Microsoft Laboratory through the *kinect* system. We selected the eighth group of throwing and the ninth group of lifting arms two movements to carry on our research. The segmentation of both actions is shown in Figure 4. As mentioned above, the method of collection is to record the three-dimensional real-time coordinates of the human joints as shown in Figure 1(a).

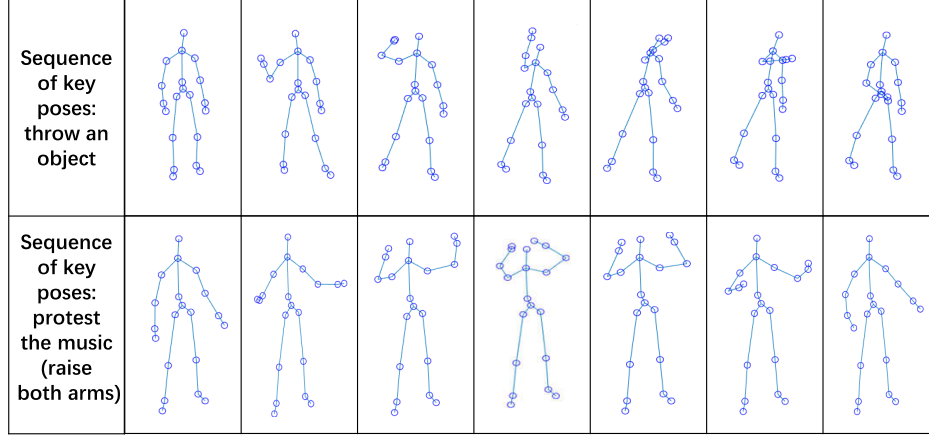


Figure 4. Action Segmentation: we use the MSRC-12 dataset collected by the Cambridge Microsoft Lab. We segment a complete action from the whole, the upper panel shows a segmentation of the "throw" action. The lower panel shows the "raising both arms" action.

We calculated the angle of the torso on each joint point through the feature extraction of the first part. The 1 ~ 9 represents the relative angle between the limbs of the upper human body, and 10 ~ 16 indicates the relative angle between the limbs of the lower body, and the relative angle between the limbs of the lower body is 17 ~ 22.

two kinds of motion patterns. Segment the movement for each action and calculate the standard deviation of the torso angle on each joint point during each action period. We get the samples in table III. Considering the importance of this part of the study and the layout, we only put sample data of the upper limb in the table.

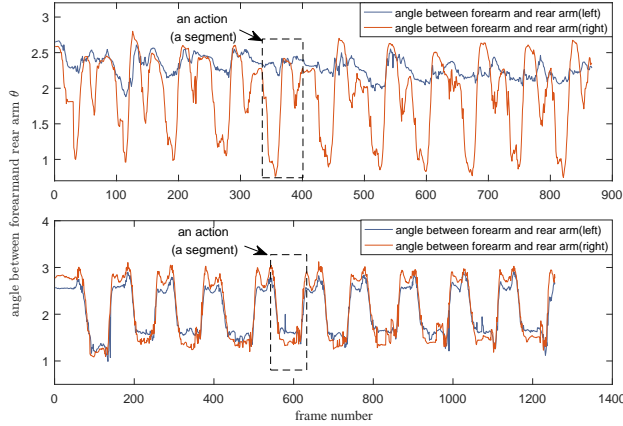


Figure 5. The curve of the elbow angle changes. It is the angle between the forearm and the back arm of the elbow. The picture above is the action "throw", the lower figure shows the raising both arms movement. The motion amplitude of the left arm of the throwing action is much smaller than that of other limbs.

Figure 5 shows the change of the angle between the left and right arms of the two movements at the elbow. As can be seen from the figure, the curve periodically renders 10 sets of actions. Further, it can be seen that the magnitude of the left arm movement changes during the throwing motion, which is much smaller than the other three curves. Therefore, the motion amplitude of the two arms can be used as a basis to distinguish the

B. Results

We processed 13 sets of throwing action data and 16 raising both arms movements, and obtained 130 groups of throwing samples and 160 groups of raising both arms samples. Select 70 groups and 90 groups respectively as training sets, and the remaining 60 groups and 70 groups as test sets. The penalty factor c and kernel function parameter σ of *svm* model are determined by cross validation and quantum genetic algorithm, respectively. In this paper, we did not reduce the dimensionality of the data mainly for two reasons. Firstly, in order to make the program have a better scalability. It can extend from the upper limb action to the whole body action classification. Secondly, in our classification algorithm operation, the time and the computing complexity is acceptable for 22-dimensional data. Thus, we take the sample directly into the SVM for learning. The throwing action is labeled as 1, the raising both arms action is labeled as 2.

During the calculation process, we set the population size to 80 and the quantum bit length to 60 bits for QGA. As the speed of convergence is very fast, the number of evolution is 5. The search range of penalty factor C is set to $[2^{-2}, 2^4]$. For the kernel function σ , the range is set to $[2^{-4}, 2^4]$. We also provide the classification accuracy results for different generations of quantum genetic algorithm. The results are shown in Figure IV. It can be seen quantum genetic algorithm converges after two generations. Due to the fast convergence speed, we set $\epsilon = 0$

Table III. action sample

(a)throw an object										
Sample	Standard Deviation	σ_8	σ_9	σ_{10}	σ_{11}	σ_{12}	σ_{13}	σ_{14}	σ_{15}	σ_{16}
1		0.0791	0.1809	0.1701	0.0545	0.1133	0.1418	0.1853	0.4574	0.1983
2		0.1356	0.1904	0.1337	0.1027	0.0797	0.0722	0.1530	0.5066	0.1741
3		0.1140	0.2099	0.1616	0.0721	0.1173	0.1236	0.1967	0.4215	0.1908
4		0.1064	0.1820	0.1496	0.0401	0.0844	0.1619	0.2261	0.5204	0.1079
5		0.1044	0.1997	0.1373	0.0686	0.0804	0.0655	0.2213	0.4555	0.1740
6		0.1242	0.2411	0.1405	0.0729	0.0654	0.0619	0.1560	0.4440	0.0589
7		0.0822	0.2239	0.1603	0.0664	0.0533	0.0523	0.1779	0.5497	0.2006
8		0.0612	0.1540	0.1500	0.0836	0.0326	0.0857	0.1566	0.4372	0.2104
9		0.1053	0.1563	0.1130	0.0614	0.0629	0.0632	0.1522	0.5194	0.2687
10		0.0796	0.1703	0.1492	0.0572	0.1021	0.1729	0.2052	0.5719	0.2363

(b)protest the music										
Sample	Standard Deviation	σ_8	σ_9	σ_{10}	σ_{11}	σ_{12}	σ_{13}	σ_{14}	σ_{15}	σ_{16}
1		0.0785	0.0756	0.1379	0.3057	0.3417	0.1553	0.3436	0.3815	0.3574
2		0.0820	0.0817	0.1405	0.3288	0.4015	0.1398	0.3957	0.4192	0.1391
3		0.1138	0.1019	0.1989	0.2674	0.4424	0.1239	0.3084	0.4681	0.2319
4		0.1166	0.0959	0.1994	0.3255	0.3720	0.1303	0.3390	0.4535	0.1699
5		0.1090	0.1042	0.2003	0.3672	0.4134	0.1458	0.3508	0.4613	0.1605
6		0.1264	0.0923	0.1965	0.3016	0.4658	0.2046	0.3319	0.4719	0.1652
7		0.1274	0.1051	0.2083	0.3122	0.3994	0.1314	0.3507	0.5100	0.1219
8		0.1441	0.1002	0.2359	0.3018	0.5652	0.1928	0.3320	0.6320	0.2010
9		0.1232	0.0965	0.2082	0.3006	0.5396	0.1776	0.3276	0.5996	0.1692
10		0.1042	0.0756	0.1763	0.3153	0.4164	0.1237	0.3272	0.4609	0.1611

By calculating the standard deviation of the angles of the joints, we get 10 groups of samples for each kind of action in the table.

Table IV. The parameters obtained through the cross validation (CV) and the quantum genetic algorithm (QGA), respectively.

	penalty factor C	kernel function parameter σ	generation	accuracy	time(S)
cross validation	0.25	0.0625	×	93.85%	4.38
quantum genetic algorithm	15.839	0.155	1	93.85%	6.83
	10.831	0.080	2	96.15%	12.29
	10.831	0.080	3	96.15%	17.62
	10.831	0.080	5	96.15%	28.17

without considering the time complexity brought by the convergence speed in this experiment. The quantum genetic algorithm increased the classification accuracy by nearly 2.5% in comparison with the conventional SVM. From Table IV, the reason why the quantum genetic algorithm can find the optimized C and σ is that it cut the parameters space into 2^{60} blocks and searched for the parameters subtly. For the cross validation approach, a very large amount of computation will be needed to achieve such an accuracy. Due to the characteristics of parallel computation, the quantum genetic algorithm only consumes less than three times the length of time and ac-

complishes the goal. To make the results more intuitive, we refine the results by confusing matrices in Table V(a) and Table V(b).

The confusion matrix is shown in Table V. The solution space of cross verification search is limited and the result is farther from the optimal solution. The quantum genetic algorithm, by the characteristics of quantum parallelism, extends the solution space under the same time complexity, which brings better results. By examining the angles of the joints and limbs to identify the human behavior pattern, the correct rate of human action recognition can achieve an accuracy of above 95%. This proves

Table V. Confusion Matrix

(a)QGA

\	Throw	Raise both arms	Accuracy
Throw	60	0	100%
Raise both arms	5	65	92.86%

(b)CV

\	Throw	Raise both arms	Accuracy
Throw	60	0	100%
Raise both arms	8	62	88.57%

the effectiveness of our approach.

IV. CONCLUSIONS

Due to the parallel characteristics of quantum algorithm, we succeeded in improving the accuracy of SVM classification without much difference of time complexity. This paper can be considered as a good example

of the combination of QGA and classification algorithm. The quantum-inspired algorithm can be used in combination with other algorithms. Next, we will work on more complex actions and incorporate new features to further improve the accuracy of SVM classification.

This paper presents a new method of representing and classifying human actions by using the quantum generic algorithm to optimize the SVM. We extracted the joints' angles from the skeleton joints' positions to represent the human stick figure. In this way, the dimensionality was reduced by 1/3. By reducing the dimensionality of samples and increasing the efficiency of computation, we achieved a higher classification accuracy in comparison with the conventional SVM method.

V. ACKNOWLEDGEMENT

This research has been funded by the National Key Research and Development Plan under the grant 2017YFC0804401.

-
- | | |
|---|---|
| <p>[1] S. Chernbumroong, S. Cang, and H. Yu, decision support systems 66, 61 (2014).</p> <p>[2] D. Abowd, A. K. Dey, R. Orr, and J. Brotherton, Virtual Reality 3, 200 (1998).</p> <p>[3] P. Woznowski, D. Kaleshi, G. Oikonomou, and I. Craddock, Computer Communications 89, 34 (2016).</p> <p>[4] L. L. Presti and M. La Cascia, Pattern Recognition 53, 130 (2016).</p> <p>[5] J. K. Aggarwal and M. S. Ryoo, ACM Computing Surveys (CSUR) 43, 16 (2011).</p> <p>[6] B. Seddik, S. Gazzah, and N. E. B. Amara, Iet Computer Vision 11, 530 (2017).</p> <p>[7] S. Gaglio, G. L. Re, and M. Morana, IEEE Transactions on Human-Machine Systems 45, 586 (2015).</p> <p>[8] C. Cortes and V. Vapnik, Machine Learning 20, 273 (1995).</p> <p>[9] M. Mosca, Physics 43, 309 (2008).</p> <p>[10] M. A. Nielson and I. L. Chuang, <i>Quantum Computation and Quantum Information: 10th Anniversary Edi-</i></p> | <p><i>tion</i> (Cambridge University Press, 2011) pp. 1–59.</p> <p>[11] N. Jones, Nature 498, 286 (2013).</p> <p>[12] A. K. Lenstra, Designs Codes & Cryptography 19, 101 (2000).</p> <p>[13] X. Zhang and D. Jiang, Shock and Vibration,2017,(2017-02-15) 2017, 1 (2017).</p> <p>[14] F. Wei, L. Min, W. Gang, J. Xu, B. Ren, and G. Wang, in <i>International Conference on Ubiquitous Robots and Ambient Intelligence</i> (2016) pp. 997–1002.</p> <p>[15] P. Chen, L. Yuan, Y. He, and S. Luo, Neurocomputing 211, 202 (2016).</p> <p>[16] J. G. Zhou and Y. Y. An, in <i>International Conference on Advanced Computer Theory and Engineering</i> (2010) pp. V4–553 – V4–556.</p> <p>[17] F. D. Xie, W. M. Yang, D. H. Qiu, and Y. Li, Advanced Materials Research 1065-1069, 199 (2015).</p> <p>[18] S. Fothergill, H. Mentis, P. Kohli, and S. Nowozin, in <i>Proceedings of the SIGCHI Conference on Human Factors in Computing Systems</i> (ACM, 2012) pp. 1737–1746.</p> |
|---|---|